ARTICLE IN PRESS

Available online at www.sciencedirect.com

SCIENCE DIRECT®

Building and Environment ▮ (▮▮▮▮) ▮▮▮–▮▮▮

BUILDING AND ENVIRONMENT

www.elsevier.com/locate/buildenv

Optimal control of building HVAC&R systems using complete simulation-based sequential quadratic programming (CSB-SQP)

Jian Sun*, Agami Reddy

Department of Civil, Architectural and Environment Engineering, Drexel University, 3141 Chestnut Street, Philadelphia, PA 19104, USA

Received 3 February 2004; accepted 24 June 2004

Abstract

This paper presents a general and systematic methodology, termed complete simulation-based sequential quadratic programming (CSB-SQP), for determining the optimal control of building HVAC&R systems. This approach allows the coupling of a detailed simulation program with an efficient optimization method, namely the sequential quadratic programming (SQP) algorithm. This approach allows the use of accurate component models of the system as against empirical models as currently used, while providing efficient optimal solutions to be determined. We develop the mathematical basis of the methodology and apply it to a simple cooling plant system to illustrate the accuracy, efficiency and robustness of this method. The issue of implementing such an optimization under real-time control is also discussed.

Keywords: Optimization; HVAC&R; Simulation; SQP; Control; Cooling plants

1. Introduction

Over the last three decades, there has been considerable amount of interest in developing effective building operation strategies to achieve maximum energy savings. Various optimal or near-optimal operating strategies, associated both with and without building thermal mass and thermal energy storage systems, have been investigated for different types of building HVAC&R systems. The control strategy to optimally operate building HVAC&R systems can be divided into two broad categories whose relationship is shown in Fig. 1 [1]:

(1) *Deciding on best operating mode*: This involves determining the type and the number of equipment to be run (such as chiller, cooling tower, condenser water and chilled water pump, etc.) which would meet the load and comfort requirements while consuming the minimum energy. Such a scheduling problem can be viewed as an integer-programming problem with the control variables being the specific combination of equipment to be operated. An important operating mode is the sequencing of chillers, cooling towers and pumps. The sequencing defines the order and conditions associated with bringing equipment online or moving them offline.

(2) *Deciding on optimal set point for local-controllers*: This is generally a nonlinear programming problem. The potential energy saving from optimal set point control is due to the fact that at any given time and operating mode, cooling load may be met by different combination of the control variables set points. However, only one set of control set point results in minimum energy consumption of the system. As is well known [1], there exists a tradeoff between energy consumption of different equipment in a HVAC&R system that in its wide sense consists of a primary plant and air distribution sub-systems. For example, consider the condenser water loop. Increasing the fan speed of the cooling tower

*Corresponding author. Tel.: +1-215-895-2736.
E-mail address: js336@drexel.edu (J. Sun).

0360-1323/$ - see front matter © 2004 Elsevier Ltd. All rights reserved.
doi:10.1016/j.buildenv.2004.08.011

Nomenclature

AU_{cd}, AU_{ev}	*con*denser, *ev*aporator overall heat-transfer coefficient, W/°C
COP	*c*oefficient *o*f *p*erformance
M_{air}	cooling water *air* mass flow rate, kg/s
M_{chw}	*ch*iller *w*ater *m*ass flow rate, kg/s
M_{cw}	*c*ooling *w*ater *m*ass flow rate, kg/s
m_R	*r*efrigerant *m*ass flow rate, kg/s
P_{ch}	*ch*iller *p*ower consumption, kW
P_{fan}	cooling tower *fan* power consumption, kW
P_{pump}	condenser water *pump* power consumption, kW
P_{loss}	electromechanical *loss*es, kW
Q_{cd}	*con*denser heat transfer, kW
Q_{ev}	*ev*aporator heat transfer (cooling load), kW
T_{cdwi}	*con*denser *w*ater *i*nlet *t*emperature, °C
T_{cdwo}	*con*denser *w*ater *o*utlet *t*emperature, °C
T_{chwi}	*ch*illed *w*ater *i*nlet *t*emperature, °C
T_{chwo}	*ch*illed *w*ater *o*utlet *t*emperature, °C
T_{ctai}	*c*ooling *t*ower *a*ir *i*nlet *t*emperature, °C
T_{ctao}	*c*ooling *t*ower *a*ir *o*utlet *t*emperature, °C
T_{wb}	ambient *w*et *b*ulb *t*emperature, °C
T_{cwi}	*c*ooling *w*ater *i*nlet *t*emperature, °C
T_{cwo}	*c*ooling *w*ater *o*utlet *t*emperature, °C
γ_{pump}	relative speed of the condenser water *pump* (actual/rated)
γ_{fan}	relative speed of the cooling tower *fan* (actual/rated)

increases fan power, but reduces chiller compressor power because the condenser water inlet temperature is decreased. In the chiller water loop, increasing the chilled water set point temperature reduces chiller power but increases pump power because a greater flow rate is needed to meet the load. Increasing the building supply air set point increases fan power but decreases chilled water pump power. For air distribution loops with variable air volume (VAV) system, increasing the supply air set point reduces chiller power since the required cooling decreases, but on the other hand increases the fan power.

Some studies used a different approach to solve the problem of determining an optimal control strategy. The state of knowledge to date relating to the operational strategies that use building HVAC&R system dynamics and interaction for reducing energy use is summarized by Hackner et al. [2], while Septhmann [3] investigated the optimized control sequencing of multiple chillers using an analysis involving part load energy characteristic for individual chillers. Some common control strategies for minimizing the electrical energy costs of a centrifugal chiller plant which consider the tradeoff among various energy-consuming equipments are described in [4]. The study by Cumali [5] applied global optimization techniques to determine optimal control and operation strategies in real time on a large scale for several buildings. His study found: (i) that the projected and/or augmented Lagrange multiplier methods did not perform well because of the equality constraints used in the problem formulation; and (ii) the generalized reduced gradient method appears to provide consistent results if one starts with a feasible solution. Braun [6] proposed both optimal and near-optimal algorithms for calculating the best values of the independent control variables based on the assumption that the energy cost of each equipment and that of the whole system can be well approximated by a quadratic functions. An algorithm based on an open-loop control equation in terms of the total chiller-water cooling load to determine the near-optimal operating sequence of cooling towers is proposed in [7], while Olson [8] developed an optimization model for a chiller plant with three chillers and four cooling tower cells, and solved it by using sequential quadratic programming along with heuristic approach to explore discrete equipment alternatives for deciding on the best operating mode of the entire system. His results show that the computation can be reduced significantly by this approach. Austin [9] proposed a method of establishing part load energy characteristics for individual chillers, which was used to better control multiple chiller plants. Koeppel et al. [10] used a global optimization algorithm (specifically simulated

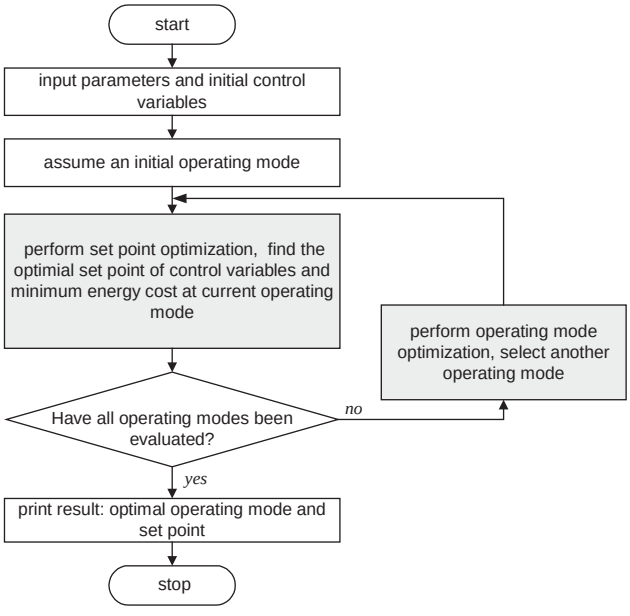

Fig. 1. Two-level optimization.

annealing) to determine the optimal supervisory control strategies for an absorption chiller system. The results indicated that simulated annealing is a robust method for optimization which can accommodate non-linear performance characteristics and discontinuous control functions. Chow [11] proposed a new concept of integrating neural network and genetic algorithm for system-based control of an absorption chiller system.

2. Problem statement and objective

The system optimization problem can be viewed as an extension of the system simulation problem. Effectively meshing optimization algorithms with system simulation requires more than just an optimization code and a system simulator containing the system model. Most studies have treated the simulation as a "black box" from which function and constraint values can be obtained for a set of control variables. A general way is to implement a complete simulation in the inside loop (deciding on optimal set point) for evaluating the objective function and constraints of the optimization problem. The control variables are specified by the outside optimization loop. Most studies adopt a system optimization strategy that involved fitting simple models to experimental data, or to data generated from a rigorous model, and then applying an optimization algorithm only to the simplified models. This approach can usually guarantee convergence of even the most complex optimization algorithm in the outside loop (deciding on best operating mode). However, a non-optimal solution could be obtained. This is because the termination criteria for simulation and optimization problems are different. The former is based on function values, while the later is based on the gradient of the objective function and constraints. Using the simplified models that have function gradients different from those of the rigorous models can lead to a situation where the optimality conditions are satisfied at non-optimal points.

Building HVAC&R systems are often large complicated nonlinear systems that consist of many strongly coupled subsystems. The accuracy and reliability of optimal supervisory control strategies depend strongly on the accuracy of mathematical models for describing the system and the method used for finding the optimal control variables. Hence, it is necessary to apply the rigorous model in the inside simulation loop. The disadvantage of this approach is that the rigorous model is often difficult to differentiate analytically. Sometimes the derivative information can only be obtained by perturbation methods that are extremely time consuming, and hence, hinder the implementation of advanced optimization algorithms in the outside loop. So the direct search method which does not use derivative information, such as the Hooke and Jeeves method, random walk algorithm, etc., is often used to solve for optimization even though it is less computationally efficient.

This paper will develop a systematic methodology for modeling the set point optimization problem and solving it by effectively applying a derivative-based optimization algorithm (namely, sequential quadratic programming [12]) coupled with a rigorous simulation model that can guarantee both accuracy and convergence. The efficient strategy to evaluating the function and derivative information from the complete modular-based system simulation is also presented in this paper. The algorithm to couple the complete modular-based system simulation and sequential quadric programming method is described. The accuracy, efficiency and robustness of this methodology are illustrated by applying it to a simple cooling plant system. How to implement the proposed optimization strategy under real-time control is also addressed.

3. Mathematical modeling

3.1. Description of system layout

Fig. 2 depicts a typical building HVAC&R system that consists of two sub-systems: (i) cooling plant, and (ii) air distribution system. The cooling plant consists of two water loops: condenser water loop and chilled water loop. These include chillers, cooling towers, condenser water pumps, chilled water pumps, and auxiliary equipment. Chillers are often arranged in parallel and water pumps are often operated by dedicated controls which cycle each pump on and off in conjunction with the chiller that it serves. The cooling tower cells are also in parallel and share a common sump with individual multi-speed or variable speed fans. The air distribution system includes air-handing units, terminal units and some auxiliary equipment. An air-handing unit consists of a cooling coil, dampers, fan and controls. The cooling load from the building is carried by the cold airflow through the cooling coil, where it is transferred to chilled water then to the chiller plant. There it is passed on to the condenser water, so that it might finally be rejected to the ambient air.

Because the plant optimization problem is an extension of the plant-simulation problem, the solution method for the simulation process will significantly affect the optimization process. At the system level, the simulation process involves solving a set of nonlinear equations that can be organized in different ways. Two main methods, equation-oriented simulation and sequential modular simulation [13] are used widely in engineering. The sequential modular simulation approach represents the system as a collection of

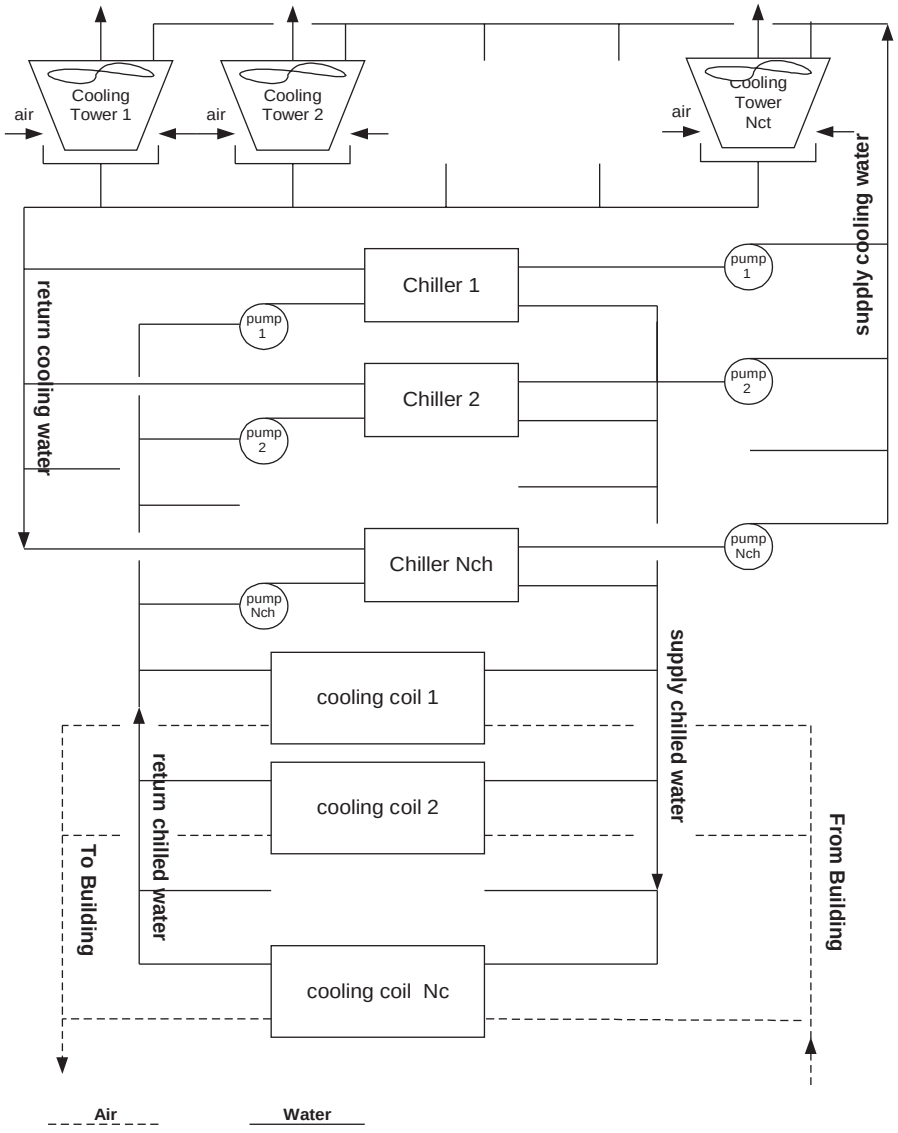

Fig. 2. Schematic of a typical building HVAC&R system.

modules in which the equations representing each subsystem or piece of equipment are coded so that a module may be used in isolation from the rest of the plant. The equation-oriented simulation is to combine all the equations into a large system of nonlinear equations, which provides flexibility for implementing an efficient and sophisticated optimization algorithm. However, it is difficult to build a complex simulator to derive the solution procedure and handle large sets of equations simultaneously. Additionally, the computation cost of this approach often becomes unacceptable. Although less flexible, the sequential modular simulation approach is easy to construct and to understand while allowing the means of incorporating new modules for modeling more complex system without changing the overall solution strategy. Thus, the sequential modular simulation is much more widely used by building HVAC&R system-simulation software.

3.2. Definition of a module

A module is defined as a model of an individual element in a system that can be coded, analyzed, and debugged by itself. The general diagram (Fig. 3) for a module consists of an input variable vector (**u**), input parameter vector (**p**), output variable vector (**y**) and the mathematical relationship between the input and output (f).

In a building HVAC&R system, certain software programs (such as TRNSYS [14], DOE-2 [15]) use the sequential modular-simulation algorithm and define modules for chiller, cooling tower, cooling coil, heat exchanger, pump, fan, flow mixer, valve and so on. For

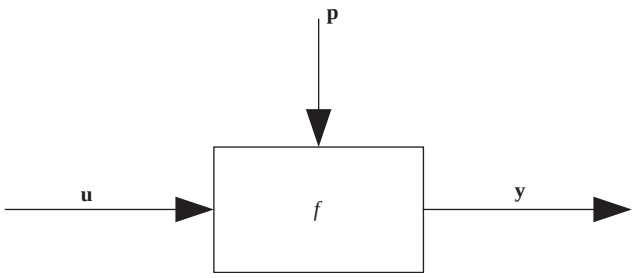

Fig. 3. A general module diagram.

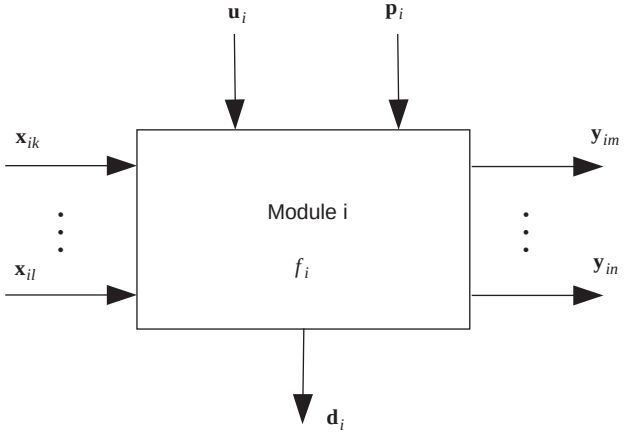

Fig. 4. Schematic of an elementary module.

example, a centrifugal chiller [16] can be defined following Fig. 3 as

$$\mathbf{u} = [M_{\text{chw}}, T_{\text{chwi}}, M_{\text{cw}}, T_{\text{cdwi}}],$$
$$\mathbf{y} = [Q_{\text{ev}}, T_{\text{chwo}}, Q_{\text{cd}}, T_{\text{cdwo}}, m_{\text{R}}, P_{\text{ch}}, \text{COP}],$$
$$\mathbf{p} = [\text{AU}_{\text{ev}}, \text{AU}_{\text{cd}}, P_{\text{loss}}, \ldots].$$

where the symbols are defined in the nomenclature. For building HVAC&R system optimization, a more detailed definition of a module is needed (see Fig. 4). First, we need to distinguish between the input connection variable $\mathbf{x}$ and input control variable $\mathbf{u}$. Second, we need to distinguish between the output connection variable $\mathbf{y}$ linking this module to other modules, and output-dependent variable $\mathbf{d}$ which is used to evaluate the objective function and/or the constraints. The connection relationship between different modules also needs to be specified in the definition of the module. Thus, the general module diagram for the system optimization is given by Fig. 4 for module i assuming modules $k \ldots 1$ to be upstream and modules $m \ldots n$ to be downstream, $\mathbf{X}_i =$ Input connection vector of module i, $\mathbf{X}_i = [\mathbf{x}_{ik} \ \ldots \ \mathbf{x}_{il}]^{\text{T}}$. The connection vector from module k to module i ($\mathbf{x}_{ik}$) is re-expressed as $\mathbf{x}_{ik} = \mathbf{x}_i^1 = [x_{i,1}^1 \ x_{i,2}^1 \ldots x_{i,N_k}^1]^{\text{T}}$ in order to account for different quantities such as temperatures, mass flow rates, enthalpies, etc.

Similarly,

Connection vector from module l to module $i = \mathbf{x}_i^{N_{i,\text{in}}} = [x_{i,1}^{N_{i,\text{in}}} \ x_{i,2}^{N_{i,\text{in}}} \ \ldots \ x_{i,N_l}^{N_{i,\text{in}}}]^{\text{T}}$,

$N_{i,\text{in}}$ is the number of input connection variables for module i.

Finally, $\mathbf{X}_i = [\mathbf{x}_i^1 \ \mathbf{x}_i^2 \ \ldots \ \mathbf{x}_i^{N_{i,\text{in}}}]^{\text{T}}$ $(k, l \in \{1, 2 \ \ldots \ N\}$ and $k, l \neq i)$,

N is the total number of modules in the system.

Similarly,

$\mathbf{Y}_i =$ Output connection vector of module i,

$\mathbf{Y}_i = [\mathbf{y}_{im} \ \ldots \ \mathbf{y}_{in}]^{\text{T}} = [\mathbf{y}_i^1 \ \ldots \ \mathbf{y}_i^{N_i,\text{out}}]^{\text{T}}$ $(m, n \in \{1, 2 \ldots N\}$ and $m, n \neq i)$,

Connection vector from module i to module $m = \mathbf{y}_i^1 = [y_{i,1}^1 \ y_{i,2}^1 \ \ldots \ y_{i,N_m}^1]^{\text{T}}$,

Connection vector from module i to module $n = \mathbf{y}_i^{N_{i,\text{out}}} = [y_{i,1}^{N_{i,\text{out}}} \ y_{i,2}^{N_{i,\text{out}}} \ \ldots \ y_{i,N_n}^{N_{i,\text{out}}}]^{\text{T}}$,

$N_{i,\text{out}}$ is the number of output connection variables for module i.

$\mathbf{u}_i =$ Design or control variable vector of module $i = [u_{i,1} \ \ldots \ u_{i,N_u}]^{\text{T}}$,

N_u is the number of input control variables for module i.

$\mathbf{p}_i =$ Physical parameter variable vector specific to system representing module $i = [p_{i,1} \ \ldots \ p_{i,N_p}]^{\text{T}}$,

N_p is the number of parameters for modules i.

$\mathbf{d}_i =$ Dependent variable vector of module $i = [d_{i,1} \ \ldots \ d_{i,N_d}]^{\text{T}}$,

N_p is the number of dependent variables for module i.

When the parameter variables $\mathbf{p}_i$ are fixed for each module i, the output variables including the output connection variables $\mathbf{Y}_i$ and dependent variables $\mathbf{d}_i$ are function of input variables, including both control variables and input connection variables.

$$\mathbf{Y}_i = \mathbf{Y}_i(\mathbf{u}_i \ \mathbf{X}_i), \tag{1}$$

$$\mathbf{d}_i = \mathbf{d}_i(\mathbf{u}_i \ \mathbf{X}_i). \tag{2}$$

3.3. System and system diagram

As described in Section 3.1, a typical building HVAC&R system consists of several loops (condenser water loop, chilled water loop and air distribution loop). Fig. 5 shows an elementary modular-based topology of such a system. The large-scale building HVAC&R system can be represented by a combination of elementary modular-based diagrams. The main purpose of optimal design or control of a HVAC&R system is to save energy. The energy consumed by a HVAC&R system (usually in the form of electricity, oil and natural gas) can be viewed as the objective function of the optimization problem. The objective function J_i can be formulated for each module as a function of input

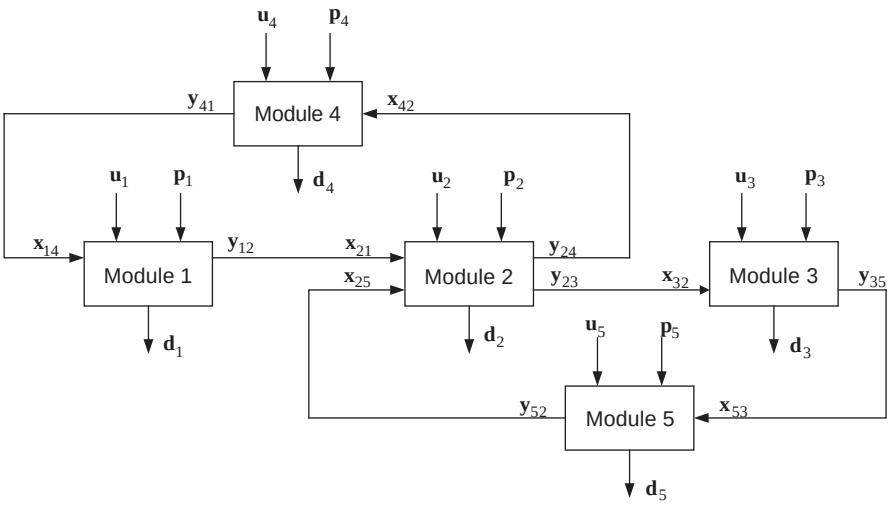

Fig. 5. Elementary topology of a building HVAC&R system.

variables.

$$J_i = J_i(\mathbf{u}_i\ \ \mathbf{d}_i) = J_i(\mathbf{u}_i\ \ \mathbf{d}_i(\mathbf{u}_i\ \ \mathbf{p}_i\ \ \mathbf{X}_i\ \ \mathbf{Y}_i)). \tag{3}$$

The total energy consumption for the whole system is the sum (or weighted sum in case of different fuels) of energy consumption of each module, and is often the performance index for system optimization.

$$J = \sum_i \mathbf{J}_i(\mathbf{u}_i\ \ \mathbf{d}_i) = J(\mathbf{u}\ \ \mathbf{d}). \tag{4}$$

The inequality constraints associated with the building HVAC&R system are mainly bound or range constraints. For example, the condenser supply temperature is bounded by upper and lower limits due to the input status and weather condition. A general equation can be used to express such an inequality as,

$$\mathbf{g}(\mathbf{u}, \mathbf{d}) \leqslant \mathbf{0}. \tag{5}$$

There are two different types of equality constraints. One is the equality constraint given by,

$$\mathbf{h}(\mathbf{u}, \mathbf{d}) = \mathbf{0}. \tag{6}$$

The other is the system constraint which represents mass and energy balance of either the various modules or at different locations of the system. These are represented by a set of algebraic equations which for module i is given by

$$f_i(\mathbf{u}_i\ \ \mathbf{X}_i\ \ \mathbf{d}_i\ \ \mathbf{Y}_i) = 0. \tag{7}$$

Substituting Eqs. (1) and (2) into Eq. (7) yields

$$f_i(\mathbf{u}_i\ \ \mathbf{X}_i\ \ \mathbf{d}_i(\mathbf{u}_i\ \ \mathbf{X}_i)\quad \mathbf{Y}_i(\mathbf{u}_i\ \ \mathbf{X}_i)) = 0 \tag{8}$$

with reduces to,

$$f_i(\mathbf{u}_i\ \ \mathbf{X}_i) = 0. \tag{9}$$

Thus, for the whole system, the system equality constraint can be expressed as

$$f(\mathbf{u}\ \ \mathbf{X}) = 0. \tag{10}$$

In order to represent the connection relationship of all modules in the system, a relevant binary matrix $\mathbf{R}$ is defined according to the system topology which specifies the relationship between output stream variable vector $\mathbf{y}_{ij}$ of one module and the input stream variable vector $\mathbf{x}_{ji}$ of the module immediately downstream.

$$\mathbf{Y} = \mathbf{R}\mathbf{X}, \tag{11}$$

where $\mathbf{X} = [\mathbf{X}_1\ \ \mathbf{X}_2\ \ \ldots\ \ \mathbf{X}_N]^{\mathrm{T}}\ \mathbf{Y} = [\mathbf{Y}_1\ \ \mathbf{Y}_2\ \ \ldots\ \ \mathbf{Y}_N]^{\mathrm{T}}$.

For example, for the system represented by Fig. 5,

$$\begin{aligned}\mathbf{X} &= [\mathbf{X}_1\ \ \mathbf{X}_2\ \ \mathbf{X}_3\ \ \mathbf{X}_4\ \ \mathbf{X}_5]^{\mathrm{T}}\\ &= [\mathbf{x}_1^1\ \ \mathbf{x}_2^1\ \ \mathbf{x}_2^2\ \ \mathbf{x}_3^1\ \ \mathbf{x}_4^1\ \ \mathbf{x}_5^1]^{\mathrm{T}}\\ &= [\mathbf{x}_{14}\ \ \mathbf{x}_{21}\ \ \mathbf{x}_{25}\ \ \mathbf{x}_{32}\ \ \mathbf{x}_{42}\ \ \mathbf{x}_{53}]^{\mathrm{T}},\end{aligned}$$

$$\begin{aligned}\mathbf{Y} &= [\mathbf{Y}_1\ \ \mathbf{Y}_2\ \ \mathbf{Y}_3\ \ \mathbf{Y}_4\ \ \mathbf{Y}_5]^{\mathrm{T}}\\ &= [\mathbf{y}_1^1\ \ \mathbf{y}_2^1\ \ \mathbf{y}_2^2\ \ \mathbf{y}_3^1\ \ \mathbf{y}_4^1\ \ \mathbf{y}_5^1]^{\mathrm{T}}\\ &= [\mathbf{y}_{12}\ \ \mathbf{y}_{24}\ \ \mathbf{y}_{23}\ \ \mathbf{y}_{35}\ \ \mathbf{y}_{41}\ \ \mathbf{y}_{52}]^{\mathrm{T}}.\end{aligned}$$

The relevant matrix $\mathbf{R}$ for the system then is given by

$$\mathbf{R} = \begin{bmatrix} \mathbf{0} & \mathbf{I} & \mathbf{0} & \mathbf{0} & \mathbf{0} & \mathbf{0} \\ \mathbf{0} & \mathbf{0} & \mathbf{0} & \mathbf{0} & \mathbf{I} & \mathbf{0} \\ \mathbf{0} & \mathbf{0} & \mathbf{0} & \mathbf{I} & \mathbf{0} & \mathbf{0} \\ \mathbf{0} & \mathbf{0} & \mathbf{0} & \mathbf{0} & \mathbf{0} & \mathbf{I} \\ \mathbf{I} & \mathbf{0} & \mathbf{0} & \mathbf{0} & \mathbf{0} & \mathbf{0} \\ \mathbf{0} & \mathbf{0} & \mathbf{I} & \mathbf{0} & \mathbf{0} & \mathbf{0} \end{bmatrix}, \tag{12}$$

where $\mathbf{I}$ is the identical matrix whose dimension is dependent on the dimension of the correspondent variable vector.

4. Proposed CBS-SQP algorithm

As discussed earlier, the optimization problem can be formulated as

$$\min \quad J(\mathbf{u},\mathbf{d}) = \sum_i J_i(\mathbf{u}_i,\mathbf{d}_i) \tag{13}$$

$$\text{s.t.} \quad \mathbf{g}(\mathbf{u},\mathbf{d}) \leqslant \mathbf{0}, \tag{13a}$$

$$\mathbf{h}(\mathbf{u},\mathbf{d}) = \mathbf{0}, \tag{13b}$$

$$f(\mathbf{u}\ \ \mathbf{X}) = 0, \tag{13c}$$

Eq. (13c) applies to the simulation problem where the function and gradient information of the objective function and constraints needs to be provided to the optimization problem. Because the gradient information is relatively difficult to obtain, the tradition approach is to use gradient-free optimization algorithms. A penalty function approach can be used to transfer the original optimization to a non-constrained problem. However, the computation cost of this approach may be unacceptable. It is necessary to find an efficient method to derive the function and gradient information from the simulation process which can be employed to reduce the computation cost, and increase accuracy and speed the convergence. Such an efficient approach to couple the module-based simulation process with a sophisticated optimization algorithm is presented below.

The dependent variable (**d**) can be calculated by the simulation program where the design or control variable (**u**) is specified. Thus, the objective and constraints given by Eq. (13a)–(13c) can be expressed as implicit functions of design or control variable (**u**). The optimization problem is rewritten as,

$$\min \quad \bar{J}(\mathbf{u}) \tag{14}$$

$$\text{s.t.} \quad \bar{\mathbf{g}}(\mathbf{u}) \leqslant \mathbf{0}, \tag{14a}$$

$$\bar{\mathbf{h}}(\mathbf{u}) = \mathbf{0}. \tag{14b}$$

For solving the above nonlinear optimization problem, two methods, namely sequential quadratic programming (SQP) and generalized reduced gradient (GRG), have proven to be most efficient and robust [17]. In this paper, we have selected SQP since it requires relatively few function and gradient evaluations, and is suitable for optimizing systems whose behavior is strongly nonlinear. The central basis of the SQP method is to converge to the solution by sequentially solving a quadratic problem that approximates the original problem.

The Lagrangian function for the above-optimization problem is given by

$$L(\mathbf{u},\boldsymbol{\alpha},\boldsymbol{\beta}) = \bar{J}(\mathbf{u}) + \boldsymbol{\alpha}^{\mathrm{T}}\bar{\mathbf{g}}(\mathbf{u}) + \boldsymbol{\beta}^{\mathrm{T}}\bar{\mathbf{h}}(\mathbf{u}). \tag{15}$$

The stationary condition for the Lagrangian of this problem with respect to the optimal conditions $\mathbf{u}^*, \boldsymbol{\alpha}^*$ and $\boldsymbol{\beta}^*$ is:

$$\nabla L(\mathbf{u}^*,\boldsymbol{\alpha}^*,\boldsymbol{\beta}^*) = \mathbf{0}. \tag{16}$$

The SQP method uses Newton's method to update $\mathbf{u}$, $\boldsymbol{\alpha}$ and $\boldsymbol{\beta}$ as follows:

$$\begin{aligned}\nabla L_{k+1}^{\mathrm{T}} &= [\nabla L(\mathbf{u}_k + \partial\mathbf{u}_k, \boldsymbol{\alpha}_k + \partial\boldsymbol{\alpha}_k, \boldsymbol{\beta}_k + \partial\boldsymbol{\beta}_k)] \\ &= \nabla L_k^{\mathrm{T}} + \nabla^2 L_k(\partial\mathbf{u}_k, \partial\boldsymbol{\alpha}_k, \partial\boldsymbol{\beta}_k)^{\mathrm{T}}.\end{aligned} \tag{17}$$

Setting $\nabla L_{k+1}^{\mathrm{T}} = 0$, we have,

$$\nabla^2 L_k \begin{pmatrix} \partial\mathbf{u}_k \\ \partial\boldsymbol{\alpha}_k \\ \partial\boldsymbol{\beta}_k \end{pmatrix} = -\nabla L_k^{\mathrm{T}}. \tag{18}$$

Also,

$$\begin{aligned}\nabla^2 L_k &\equiv \begin{pmatrix} \nabla^2_{uu}L & \nabla^2_{u\alpha}L & \nabla^2_{u\beta}L \\ \nabla^2_{\alpha u}L & \nabla^2_{\alpha\alpha}L & \nabla^2_{\alpha\beta}L \\ \nabla^2_{\beta u}L & \nabla^2_{\beta\alpha}L & \nabla^2_{\beta\beta}L \end{pmatrix}_k \\ &= \begin{pmatrix} \nabla^2\bar{J} + \boldsymbol{\alpha}^{\mathrm{T}}\nabla^2\bar{\mathbf{g}}_a + \boldsymbol{\beta}^{\mathrm{T}}\nabla^2\bar{\mathbf{h}} & \nabla\bar{\mathbf{g}}_a^{\mathrm{T}} & \nabla\bar{\mathbf{h}}^{\mathrm{T}} \\ \nabla\bar{\mathbf{g}}_a & 0 & 0 \\ \nabla\bar{\mathbf{h}} & 0 & 0 \end{pmatrix}_k,\end{aligned} \tag{19}$$

where $\bar{\mathbf{g}}_a$ is the active inequality.

The RHS of Eq. (18) can be written as,

$$\nabla L_k = (\nabla\bar{J} + \boldsymbol{\alpha}^{\mathrm{T}}\nabla\bar{\mathbf{g}}_a + \boldsymbol{\beta}^{\mathrm{T}}\nabla\bar{\mathbf{h}}\ \ \bar{\mathbf{g}}_a\ \ \bar{\mathbf{h}})_k. \tag{20}$$

So, substituting Eqs. (19) and (20) into Eq. (18) yields,

$$\begin{aligned}&\begin{pmatrix} \nabla^2\bar{J} + \boldsymbol{\alpha}^{\mathrm{T}}\nabla^2\bar{\mathbf{g}}_a + \boldsymbol{\beta}^{\mathrm{T}}\nabla^2\bar{\mathbf{h}} & \nabla\bar{\mathbf{g}}_a^{\mathrm{T}} & \nabla\bar{\mathbf{h}}^{\mathrm{T}} \\ \nabla\bar{\mathbf{g}}_a & 0 & 0 \\ \nabla\bar{\mathbf{h}} & 0 & 0 \end{pmatrix}_k \begin{pmatrix} \partial\mathbf{u}_k \\ \partial\boldsymbol{\alpha}_k \\ \partial\boldsymbol{\beta}_k \end{pmatrix} \\ &= -\begin{pmatrix} \nabla\bar{J} + \boldsymbol{\alpha}^{\mathrm{T}}\nabla\bar{\mathbf{g}}_a + \boldsymbol{\beta}^{\mathrm{T}}\nabla\bar{\mathbf{h}} \\ \bar{\mathbf{g}}_a \\ \bar{\mathbf{h}} \end{pmatrix}_k.\end{aligned} \tag{21}$$

Setting,

$$\mathbf{H} = \nabla^2\bar{J} + \boldsymbol{\alpha}^{\mathrm{T}}\nabla^2\bar{\mathbf{g}}_a + \boldsymbol{\beta}^{\mathrm{T}}\nabla^2\bar{\mathbf{h}},$$

$$\partial\mathbf{u}_k = \mathbf{u}_{k+1} - \mathbf{u}_k = \mathbf{s}_k \quad \partial\boldsymbol{\alpha}_k = \boldsymbol{\alpha}_{k+1} - \boldsymbol{\alpha}_k$$
$$\partial\boldsymbol{\beta}_k = \boldsymbol{\beta}_{k+1} - \boldsymbol{\beta}_k.$$

We get,

$$\begin{pmatrix} \mathbf{H} & \nabla\bar{\mathbf{g}}_a^{\mathrm{T}} & \nabla\bar{\mathbf{h}}^{\mathrm{T}} \\ \nabla\bar{\mathbf{g}}_a & 0 & 0 \\ \nabla\bar{\mathbf{h}} & 0 & 0 \end{pmatrix}_k \begin{pmatrix} \mathbf{s}_k \\ \boldsymbol{\alpha}_{k+1} \\ \boldsymbol{\beta}_{k+1} \end{pmatrix} = -\begin{pmatrix} \nabla\bar{J}^{\mathrm{T}} + \boldsymbol{\alpha}^{\mathrm{T}}\nabla\bar{\mathbf{g}}_a + \boldsymbol{\beta}^{\mathrm{T}}\nabla\bar{\mathbf{h}} \\ \bar{\mathbf{g}}_a \\ \bar{\mathbf{h}} \end{pmatrix}_k. \tag{22}$$

Solving the above equation iteratively for $\mathbf{u}_{k+1} = \mathbf{u}_k + \mathbf{s}_k$, $\boldsymbol{\alpha}_{k+1}$ and $\boldsymbol{\beta}_{k+1}$ should eventually lead to an optimal solution set ($\mathbf{u}^*, \boldsymbol{\alpha}^*$ and $\boldsymbol{\beta}^*$). The equation may be viewed as the Karush–Kuhn–Tucker (KKT) conditions for the following quadratic model:

$$\min_k \quad J_k + \nabla_u L_k^{\mathrm{T}}\mathbf{s}_k + \tfrac{1}{2}\mathbf{s}_k^{\mathrm{T}}\mathbf{H}_k\mathbf{s}_k \tag{23}$$

$$\text{s.t.} \quad \nabla\bar{\mathbf{h}}_k^{\mathrm{T}}\mathbf{s}_k + \bar{\mathbf{h}}_k = 0, \tag{23a}$$

$$\nabla\bar{\mathbf{g}}_k^{\mathrm{T}}\mathbf{s}_k + \bar{\mathbf{g}}_k \leqslant 0, \quad a \in \mathbf{D} \text{ where } \mathbf{D} \text{ is the active set.} \tag{23b}$$

In order to maintain the Hessian matrix $\mathbf{H}_k$ positive definite at each iteration, an approximation matrix $\mathbf{B}_k$ is used to replace $\mathbf{H}$. Broyden–Fletcher–Goldfarb–Shanno (BFGS) formula [18] can be used to update the $\mathbf{B}_k$ in the following manner:

$$\mathbf{s}_k = \mathbf{u}_{k+1} - \mathbf{u}_k, \tag{24}$$

$$\mathbf{z}_k = \nabla_u L(\mathbf{u}_{k+1}, \boldsymbol{\alpha}_{k+1}, \boldsymbol{\beta}_{k+1}) - \nabla_u L(\mathbf{u}_{k+1}, \boldsymbol{\alpha}_k, \boldsymbol{\beta}_k). \tag{25}$$

Let,

$$\theta = \begin{cases} 1 & (\mathbf{s}^k)^{\mathrm{T}}\mathbf{z}^k \geqslant \gamma(\mathbf{s}^k)^{\mathrm{T}}\mathbf{B}^k\mathbf{s}^k, \\ (1-\gamma)(\mathbf{s}^k)^{\mathrm{T}}\mathbf{B}^k\mathbf{s}^k / & \\ \quad [(\mathbf{s}^k)^{\mathrm{T}}\mathbf{B}^k\mathbf{s}^k - (\mathbf{s}^k)^{\mathrm{T}}\mathbf{z}^k] & (\mathbf{s}^k)^{\mathrm{T}}\mathbf{z}^k < \gamma(\mathbf{s}^k)^{\mathrm{T}}\mathbf{B}^k\mathbf{s}^k, \end{cases} \tag{26}$$

where $0.1 \leqslant \gamma \leqslant 0.2$

$$\mathbf{z}_k = \theta\mathbf{z}_k + (1-\theta)\mathbf{B}_k\mathbf{s}_k, \tag{27}$$

$$\mathbf{B}_{k+1} = \mathbf{B}_k + \frac{\mathbf{z}_k(\mathbf{z}_k)^{\mathrm{T}}}{(\mathbf{z}_k)^{\mathrm{T}}\mathbf{s}^k} - \frac{\mathbf{B}_k\mathbf{s}_k(\mathbf{s}_k)^{\mathrm{T}}\mathbf{B}_k}{(\mathbf{s}_k)^{\mathrm{T}}\mathbf{B}_k\mathbf{s}_k}. \tag{28}$$

In order to find a step size λ by linear search technique, an exact penalty [18] function is defined as,

$$F_\delta(\mathbf{u}) = F(\mathbf{u}) + \delta\left[\sum_i |h_i(\mathbf{u})| + \sum_i |\max\{0, g_i(\mathbf{u})\}|\right]. \tag{29}$$

The derivate information described by $\nabla\bar{J}, \nabla\bar{\mathbf{g}}$ and $\nabla\bar{\mathbf{h}}$ can be obtained from the complete simulation program. At each iterative point, a simplified system model is constructed for updating the objective function and constraints. For obtaining the simplified system model, each module of the system needs to be simplified first. For example, at iteration point ($\mathbf{u}_i^k$ $\mathbf{X}_i^k$), Taylor expansion can be used to approximate the module model

$$\begin{aligned} &\mathbf{Y}_i(\mathbf{u}_i^k + \Delta\mathbf{u}_i,\ \mathbf{X}_i^k + \Delta\mathbf{X}_i) \\ &\quad = \mathbf{Y}_i(\mathbf{u}_i^k, \mathbf{X}_i^k) + \frac{\partial\mathbf{Y}_i}{\partial\mathbf{u}_i}\Delta\mathbf{u}_i \\ &\qquad + \frac{\partial\mathbf{Y}_i}{\partial\mathbf{X}_i}\Delta\mathbf{X}_i + (\Delta\mathbf{u}_i)^{\mathrm{T}}\frac{\partial^2\mathbf{Y}_i}{\partial\mathbf{u}_i^2}\Delta\mathbf{u}_i \\ &\qquad + (\Delta\mathbf{X}_i)^{\mathrm{T}}\frac{\partial^2\mathbf{Y}_i}{\partial\mathbf{X}_i^2}\Delta\mathbf{X}_i + (\Delta\mathbf{u}_i)^{\mathrm{T}}\frac{\partial^2\mathbf{Y}_i}{\partial\mathbf{u}_i\partial\mathbf{X}_i}\Delta\mathbf{X}_i \\ &\qquad + 0\big((\Delta\mathbf{u}_i)^3, (\Delta\mathbf{X}_i)^3, \ldots\big), \end{aligned} \tag{30}$$

$$\begin{aligned} &\mathbf{d}_i(\mathbf{u}_i^k + \Delta\mathbf{u}_i,\ \mathbf{X}_i^k + \Delta\mathbf{X}_i) \\ &\quad = \mathbf{d}_i(\mathbf{u}_i^k,\ \mathbf{X}_i^k) + \frac{\partial\mathbf{d}_i}{\partial\mathbf{u}_i}\Delta\mathbf{u}_i \\ &\qquad + \frac{\partial\mathbf{d}_i}{\partial\mathbf{X}_i}\Delta\mathbf{X}_i + (\Delta\mathbf{u}_i)^{\mathrm{T}}\frac{\partial^2\mathbf{d}_i}{\partial\mathbf{u}_i^2}\Delta\mathbf{u}_i \\ &\qquad + (\Delta\mathbf{X}_i)^{\mathrm{T}}\frac{\partial^2\mathbf{d}_i}{\partial\mathbf{X}_i^2}\Delta\mathbf{X}_i + (\Delta\mathbf{u}_i)^{\mathrm{T}}\frac{\partial^2\mathbf{d}_i}{\partial\mathbf{u}_i\partial\mathbf{X}_i}\Delta\mathbf{X}_i \\ &\qquad + 0((\Delta\mathbf{u}_i)^3, (\Delta\mathbf{X}_i)^3, \ldots). \end{aligned} \tag{31}$$

The quadratic approximation model is given by

$$\begin{aligned} \Delta\mathbf{Y}_i \approx\ &\mathbf{A}_i\Delta\mathbf{u}_i + \mathbf{B}_i\Delta\mathbf{X}_i + \Delta\mathbf{u}_i^{\mathrm{T}}\mathbf{O}_i\Delta\mathbf{u}_i \\ &+ \Delta\mathbf{X}_i^{\mathrm{T}}\mathbf{P}_i\Delta\mathbf{X}_i + \Delta\mathbf{u}_i^{\mathrm{T}}\mathbf{Q}_i\Delta\mathbf{X}_i, \end{aligned} \tag{32}$$

$$\begin{aligned} \Delta\mathbf{d}_i \approx\ &\mathbf{C}_i\Delta\mathbf{u}_i + \mathbf{D}_i\Delta\mathbf{X}_i + \Delta\mathbf{u}_i^{\mathrm{T}}\mathbf{R}_i\Delta\mathbf{u}_i \\ &+ \Delta\mathbf{X}_i^{\mathrm{T}}\mathbf{S}_i\Delta\mathbf{X}_i + \Delta\mathbf{u}_i^{\mathrm{T}}\mathbf{T}_i\Delta\mathbf{X}_i \end{aligned} \tag{33}$$

and the linear approximation model is

$$\Delta\mathbf{Y}_i \approx \mathbf{A}_i\Delta\mathbf{u}_i + \mathbf{B}_i\Delta\mathbf{X}_i, \tag{34}$$

$$\Delta\mathbf{d}_i \approx \mathbf{C}_i\Delta\mathbf{u}_i + \mathbf{D}_i\Delta\mathbf{X}_i. \tag{35}$$

Although quadratic models have higher accuracy than linear models, the added computational expense often make them unsuitable. So linear approximation has been applied in this study. The coefficient matrix can be obtained by numerical perturbation.

$$\mathbf{A}_i = \frac{\partial\mathbf{Y}_i}{\partial\mathbf{u}_i} = \begin{bmatrix} \frac{\partial\mathbf{y}_i^1}{\partial u_{i,1}} & \frac{\partial\mathbf{y}_i^1}{\partial u_{i,2}} & \cdots & \frac{\partial\mathbf{y}_i^1}{\partial u_{i,n1}} \\ \cdots & \cdots & & \cdots \\ & & \frac{\partial\mathbf{y}_i^j}{\partial u_{i,k}} & \\ \frac{\partial\mathbf{y}_i^{N_{i,\mathrm{out}}}}{\partial u_{i,1}} & \frac{\partial\mathbf{y}_i^{N_{i,\mathrm{out}}}}{\partial u_{i,2}} & \cdots & \frac{\partial\mathbf{y}_i^{N_{i,\mathrm{out}}}}{\partial u_{i,N_u}} \end{bmatrix}, \tag{36}$$

where

$$\frac{\partial\mathbf{y}_i^j}{\partial u_{i,k}} = \begin{bmatrix} \frac{\partial y_{i,1}^j}{\partial u_{i,k}} & \frac{\partial y_{i,2}^j}{\partial u_{i,k}} & \cdots \frac{\partial y_{i,N_j}^j}{\partial u_{i,k}} \end{bmatrix}^{\mathrm{T}}$$

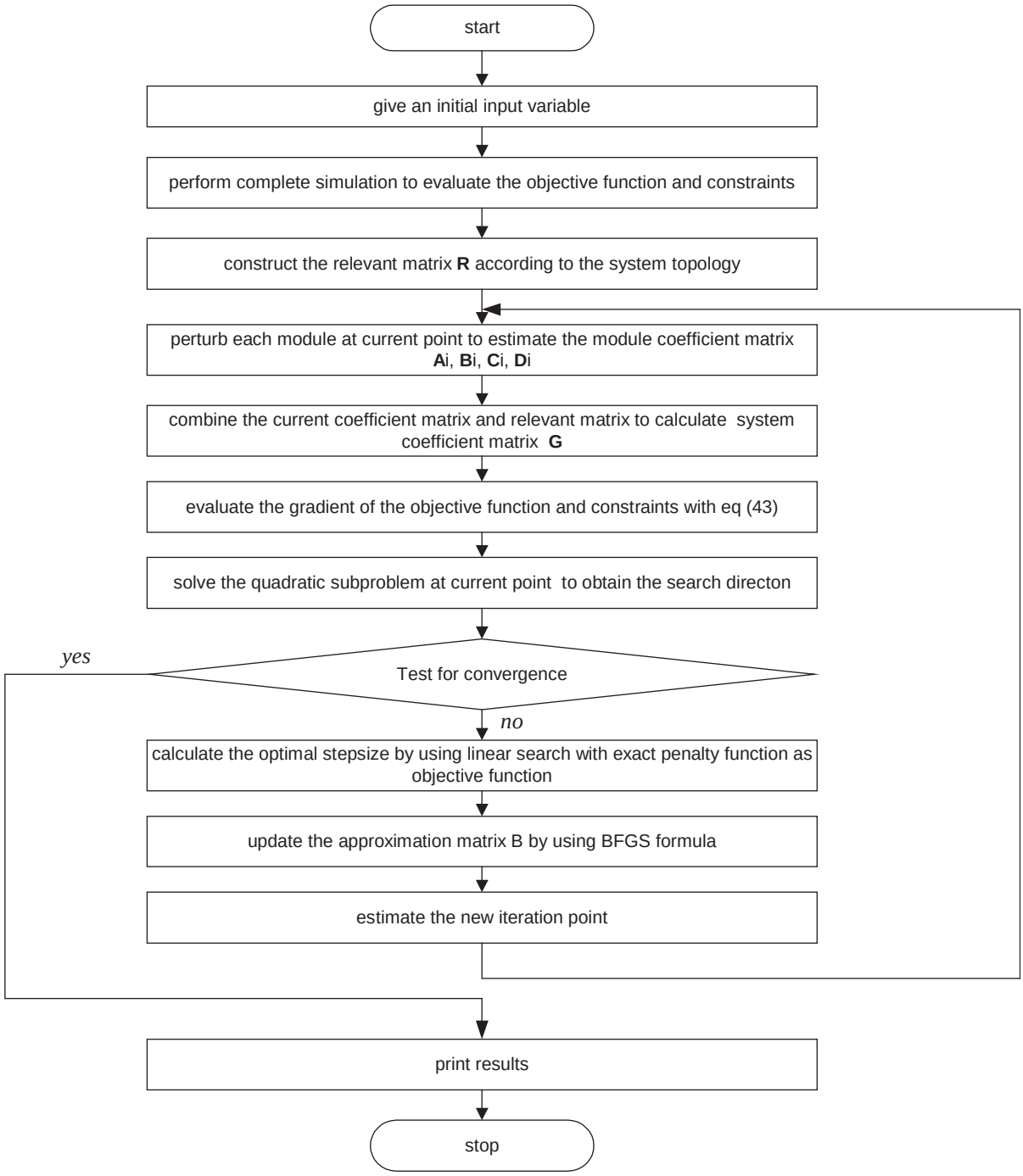

Fig. 6. Optimization procedure of CSB-SQP algorithm.

and

$$\mathbf{B}_i = \frac{\partial \mathbf{Y}_i}{\partial \mathbf{X}_i} = \begin{bmatrix} \frac{\partial \mathbf{y}_i^1}{\partial \mathbf{x}_i^1} & \frac{\partial \mathbf{y}_i^1}{\partial \mathbf{x}_i^2} & \cdots & \frac{\partial \mathbf{y}_i^1}{\partial \mathbf{x}_i^{N_{i,\text{in}}}} \\ \cdots & \cdots & & \cdots \\ & & \frac{\partial \mathbf{y}_i^j}{\partial \mathbf{x}_i^k} & \\ \frac{\partial \mathbf{y}_i^{N_{i,\text{out}}}}{\partial \mathbf{x}_i^1} & \frac{\partial \mathbf{y}_i^{N_{i,\text{out}}}}{\partial \mathbf{x}_i^2} & \cdots & \frac{\partial \mathbf{y}_i^{N_{i,\text{out}}}}{\partial \mathbf{x}_i^{N_{i,\text{in}}}} \end{bmatrix}, \quad (37)$$

where

$$\frac{\partial \mathbf{y}_i^j}{\partial \mathbf{x}_i^k} = \begin{bmatrix} \frac{\partial y_{i,1}^j}{\partial x_{i,1}^k} & \frac{\partial y_{i,1}^j}{\partial x_{i,2}^k} & \cdots & \frac{\partial y_{i,1}^j}{\partial x_{i,Nk}^k} \\ \cdots & \cdots & & \cdots \\ \frac{\partial y_{i,N_j}^j}{\partial x_{i,1}^k} & \frac{\partial y_{i,N_j}^j}{\partial x_{i,2}^k} & \cdots & \frac{\partial y_{i,N_j}^j}{\partial x_{i,Nk}^k} \end{bmatrix}.$$

Coefficient matrix $\mathbf{C}_i, \mathbf{D}_i$ can be calculated similarly. For each module of the system, a linearly approximated

model can be obtained. Thus, for the entire system, the linearized model can be expressed as,

$$\Delta \mathbf{Y} = \mathbf{A}\Delta \mathbf{u} + \mathbf{B}\Delta \mathbf{X}, \tag{38}$$

where

$$\mathbf{A} = \begin{bmatrix} \mathbf{A}_1 & & & \\ & \mathbf{A}_2 & & \\ & & \ddots & \\ & & & \mathbf{A}_N \end{bmatrix} \quad \text{and}$$

$$\mathbf{B} = \begin{bmatrix} \mathbf{B}_1 & & & \\ & \mathbf{B}_2 & & \\ & & \ddots & \\ & & & \mathbf{B}_N \end{bmatrix}.$$

The system structure and the connection between the modules can be represented by a relevant matrix $\mathbf{R}$ as shown in Eq. (12). Then, we get,

$$\Delta \mathbf{Y} = \mathbf{R}\Delta \mathbf{X}. \tag{39}$$

Combining Eqs. (38) and (39),

$$(\mathbf{R} - \mathbf{B})\Delta \mathbf{X} = \mathbf{A}\Delta \mathbf{u} \tag{40}$$

and, thus,

$$\Delta \mathbf{X} = (\mathbf{GA})\Delta \mathbf{u}, \tag{41}$$

where $\mathbf{G} = (\mathbf{R} - \mathbf{B})^{-1}$ or $\mathbf{G} = \left[(\mathbf{R} - \mathbf{B})^{\mathrm{T}}(\mathbf{R} - \mathbf{B})\right]^{-1}(\mathbf{R} - \mathbf{B})^{\mathrm{T}}$ when $(\mathbf{R} - \mathbf{B})$ is singular.

Eq. (41) can be rewritten as,

$$\Delta \mathbf{X}_i = \sum_j \mathbf{G}_{ij}\mathbf{A}_j\Delta \mathbf{u}_j. \tag{42}$$

Substituting Eq. (42) into Eq. (35) yields,

$$\Delta \mathbf{d}_i \approx \mathbf{C}_i\Delta \mathbf{u}_i + \mathbf{D}_i \sum_j \mathbf{G}_{ij}\mathbf{A}_j\Delta \mathbf{u}_j. \tag{43}$$

Now, we can calculate the derivate of $\nabla_u J(\mathbf{u},\mathbf{d})\nabla_u \mathbf{g}(\mathbf{u},\mathbf{d})\nabla_u \mathbf{h}(\mathbf{u},\mathbf{d})$ as

$$\nabla_u \psi_i(\mathbf{u},\mathbf{d}) = \frac{\partial \psi}{\partial \mathbf{u}_k} = \frac{\psi(\mathbf{u}_k + \Delta \mathbf{u}_k, \mathbf{d}_k + \Delta \mathbf{d}_k) - \psi(\mathbf{u}_k, \mathbf{d}_k)}{\Delta \mathbf{u}_k}, \tag{44}$$

where $\psi = \{J, \mathbf{g}, \mathbf{h}\}$.

The computational algorithm describing the above methodology is shown in Fig. 6.

5. Case study

5.1. Generation of control map

We shall illustrate the approach described previously by assuming a simplified building cooling system shown in Fig. 7. The system consists of one centrifugal chiller, one cooling tower and a variable speed condenser water pump. The nominal system parameters are given by Table 1.

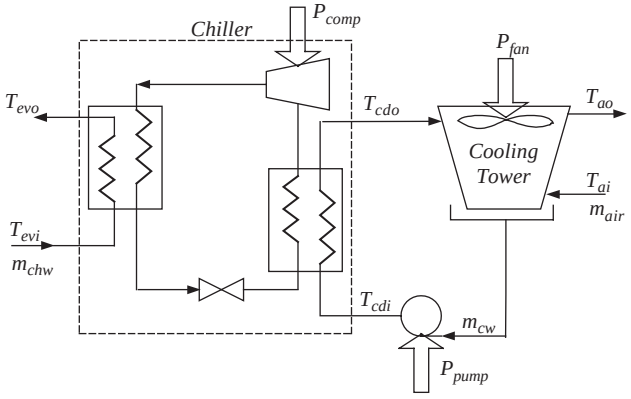

Fig. 7. Schematic of building HVAC&R system.

Table 1
Design parameters

Parameter		Value
Chiller design cooling load	Q_{ev}	1126.4 kW (320 tons)
Chilled water mass flow rate	M_{chw}	32 kg/s (507 GPM)
Chilled water inlet temperature	T_{cdwi}	15.6 °C (60 °F)
Chilled water outlet temperature	T_{chwo}	7.2 °C (45 °F)
Condenser water mass flow rate	M_{cw}	45 kg/s (713 GPM)
Condenser water inlet temperature	T_{cdwi}	24 °C (75 °F)
Condenser water outlet temperature	T_{cdwo}	29.4 °C (85 °F)
Cooling tower air flow rate	M_{air}	35 kg/s (555 GPM)

In this study, the condenser water inlet temperature T_{cdwi}, the relative speed of the condenser water pump γ_{pump} (which determines condenser water mass flow rate M_{cw}), the relative speed of cooling tower fan γ_{fan} (which determines air flow rate M_{air}) are selected as control variables. The purpose of optimization is to determine the optimal combination of these control variables under different cooling loads and ambient wet bulb temperatures T_{wb} (both of which are regarded as uncontrolled variables), which minimizes the electric power of the entire system. Thus, the performance index is the sum of the electric power of the chiller compressor P_{ch}, that of cooling tower fan P_{fan}, and that of the condenser water pump P_{pump},

$$J \equiv \sum P = P_{\mathrm{ch}} + P_{\mathrm{fan}} + P_{\mathrm{pump}}.$$

The operation of the system has to be limited to certain ranges of operating parameters to avoid practical problems such as evaporator freezing, or compressor surging. The operating ranges of the control variables

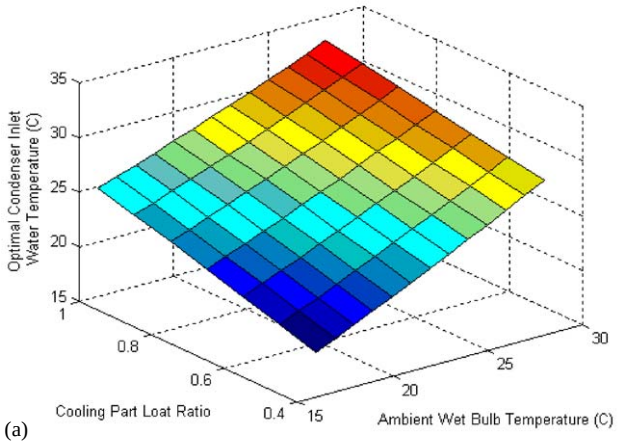

(a)

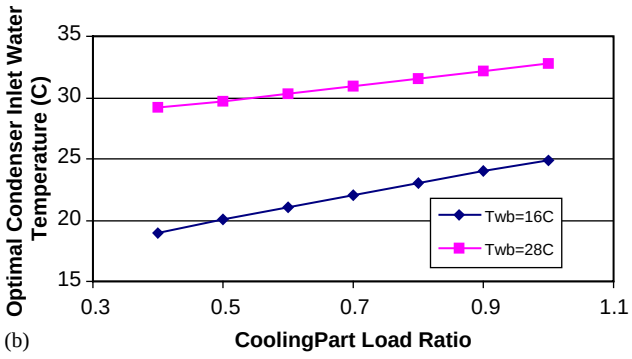

(b)

Fig. 8. (a,b) Variation of optimal condenser water inlet temperatures with wet bulb temperature and cooling load.

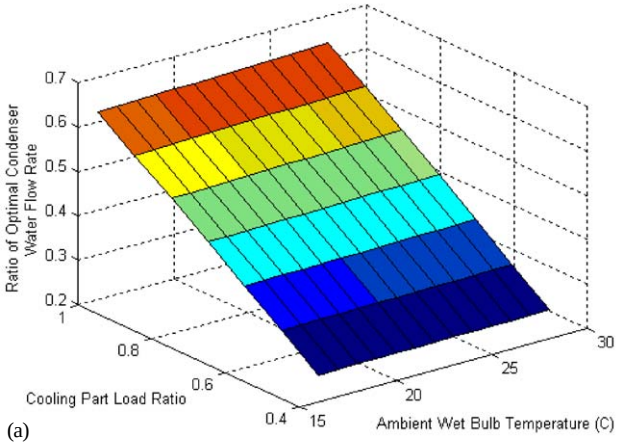

(a)

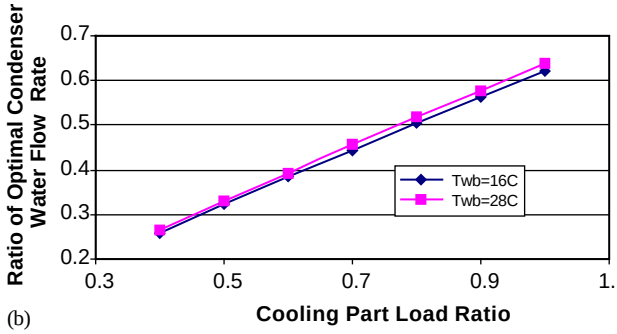

(b)

Fig. 9. (a,b) Variation of optimal condenser water flow rate with wet bulb temperature and cooling load.

form a part of the system constraints during optimization, which we have assumed to be:

(a) relative speed of condenser water pump:

$$0.4 \leqslant \gamma_{\text{pump}} \leqslant 1.0,$$

(b) relative speed of cooling tower fan:

$$0.4 \leqslant \gamma_{\text{fan}} \leqslant 1.0,$$

(c) condenser water inlet temperature:

$$\max(18\,^{\circ}\text{C}, T_{\text{wb}}) \leqslant T_{\text{cdwi}} \leqslant \max(29\,^{\circ}\text{C}, T_{\text{wb}} + 8\,^{\circ}\text{C}),$$

(d) chiller outlet temperature:

$$T_{\text{chwo}} = 7\,^{\circ}\text{C}$$

(based on the indoor humidity requirement).

The results of applying the algorithm proposed previously to the above system are summarized in Figs. 8–11 which show the variation of the optimal objective function and optimal control variables with respect to the two independent or uncontrolled variables (cooling load and ambient wet bulb temperature). We note the following trends:

(i) Fig. 8(a) and (b) shows that both cooling load and ambient wet bulb temperature have significant effect on the optimal condenser inlet water temperature. Increasing either one will increase the optimal condenser inlet water temperature.
(ii) Fig. 9(a) and (b) shows that the ambient wet bulb temperature has very little effect on the optimal condenser water flow rate. The optimal condenser water flow rate depends only on the cooling load.
(iii) Fig. 10(a) and (b) shows that the optimal cooling tower air flow rate is more sensitive to the change of cooling load than to change in ambient wet bulb temperature. Further the value of optimal cooling tower air flow rate increases with increasing cooling load or decreasing ambient wet bulb temperature.
(iv) Fig. 11(a)–(c) also suggests that the total power consumption is not very sensitive to the ambient wet bulb temperature, especially for low cooling load region.

5.2. Implementation of real-time control scheme

Given the computational complexity, it is impractical under real-time control to determine the optimal set

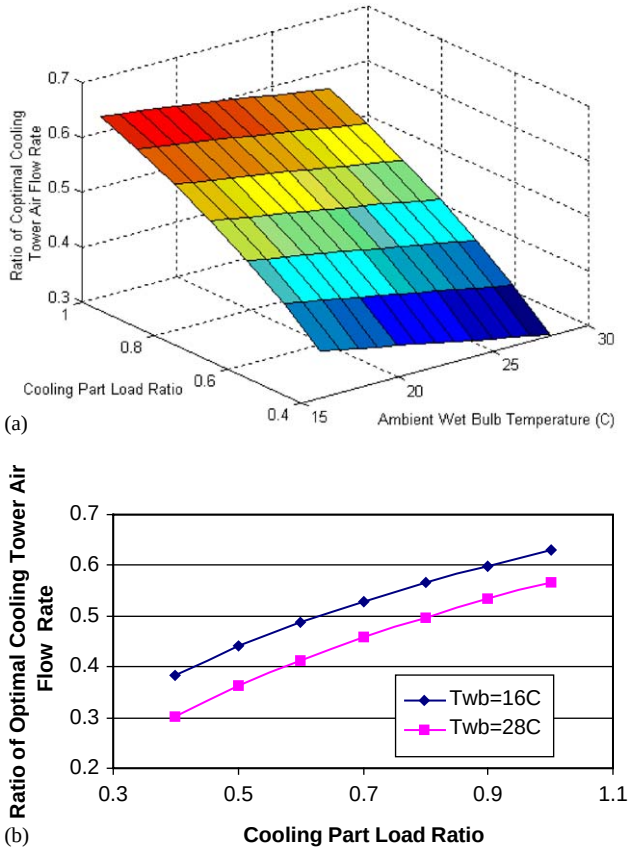

Fig. 10. (a,b) Variation of optimal air flow rate through cooling tower with wet bulb temperature and cooling load.

points by using the proposed methodology directly. Hence, it is necessary to derive simple control laws for real-time system operation. One way would be to develop regression models for each control variable from the control map of that variable. The above analysis indicates that a linear model represents the control map data quite well. Adopting a linear model as shown below:

$$\varphi = a_0 + a_1 T_{wb} + a_2(Q_{load}/Q_{load\_des}), \quad (45)$$

where T_{wb} is in °C, results in the least-squares regression coefficients for the three control variables shown in Table 2.

The total power consumption of the system can be expressed as

$$P_{tot} = x^T A x + x^T B + C,$$

where $x = [T_{wb}\ Q_{load}/Q_{load\_des}]^T$,

$$A = \begin{bmatrix} 0.006875 & 1.5258 \\ 1.5258 & -31.372 \end{bmatrix},$$

$$B = [-0.57429\ 185.9842]^T, \quad C = 14.51182,$$

model $R^2 = 99.9\%$.

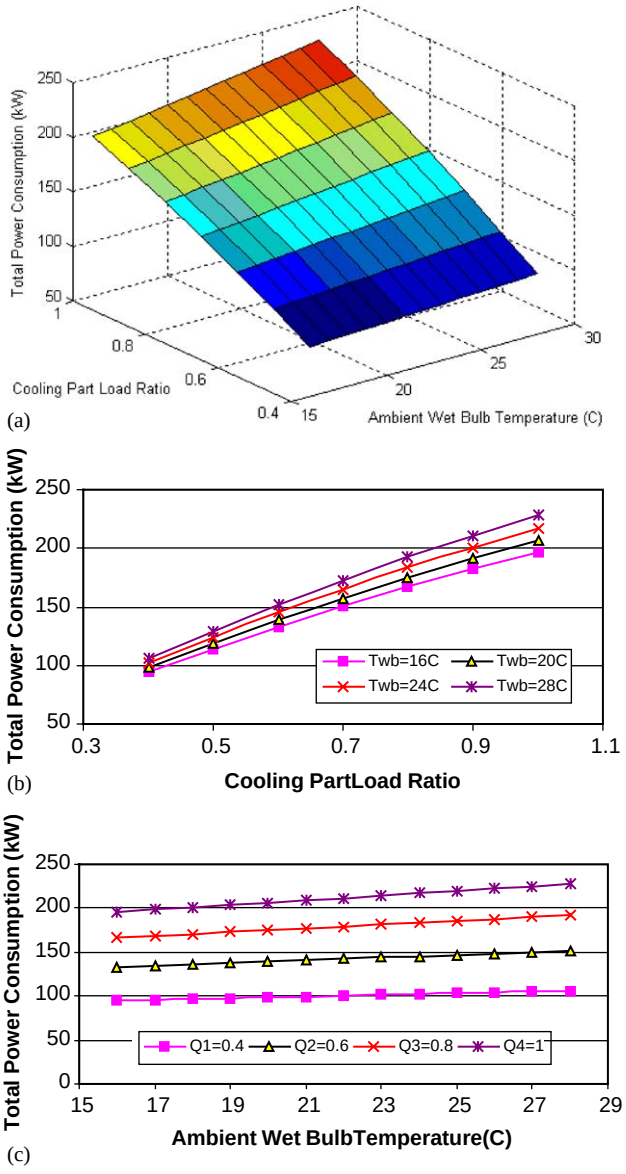

Fig. 11. (a–c) Variation of total power consumption with wet bulb temperature and cooling load.

Table 2
Coefficients of the model given by Eq. (44)

φ	a_0	a_1	a_2	Model R^2 (%)
T_{cdwi}	4.551627	0.745485	7.903648	99.4
M_{cw}/M_{cw_des}	0.321049	−0.00604	0.421814	98.8
M_{air}/M_{chw_des}	−0.00043	0.000912	0.612134	99.9

6. Conclusion and future work

This paper proposed a general methodology for optimizing the control of the existing building HVAC&R system. The same methodology could, in essence, be used for the optimal system design problem

as well. A complete simulation-based sequential quadratic programming (CSB-SQP) algorithm was developed by coupling the module-based system simulation approach with the sequential quadratic programming algorithm. A computationally efficient approach to evaluating the function and derivative information from the complete module-based system simulation is also presented. A case study of a simple cooling plant system illustrated the efficiency and robustness of this approach. This methodology can provide guidelines for engineers to optimally control the building HVAC&R system under different operating conditions. The methodology can also be easily extended to deal with more complete and complex energy systems as well.

References

[1] ASHRAE. HVAC handbook: system and equipment handbook. Atlanta, GA: ASHRAE; 2000.
[2] Hackner RJ, Mitchell JW, Beckman WA. HVAC system dynamics and energy use in existing building—part I. ASHRAE Transactions 1984; RC-84-09(2) (RP-32).
[3] Septhmann DH. Optimized control of multiple chillers. ASHRAE Transactions 1985;HI-85-16(2).
[4] Johnson GA. Optimization techniques for a centrifugal chiller plant using a programmable controller. ASHRAE Transactions 1985;HI-85-16(1).
[5] Cumali Z. Global optimization of HVAC system operations in real time. ASHRAE Transactions 1988;DA-88-23-1.
[6] Braun JE, Klein SA, Mitchell JW, Beckman WA. Methodologies for optimal control to chilled water systems without storage. ASHRAE Transactions 1989;95(1).
[7] Braun JE, Diderrich GT. Near-optimal control of cooling towers for chilled-water systems. ASHRAE Transactions 1990;96(2): 806–13.
[8] Olson RT, Liebman S. Optimization of a chilled water plant using sequential quadratic programming. Engineering Optimization 1990;15:171–91.
[9] Austin SB. Optimum chiller loading. ASHRAE Journal 1991; 33(7).
[10] Koeppel EA, Klein SA, Mitchell JW, Flake BA. Optimal supervisory control of an absorption chiller system. International Journal of HVAC& R Research 1995;1(4):325–42.
[11] Chow TT, Zhang GQ, Lin Z, Song CL. Global optimization of absorption chiller system by generic algorithm and neural network. Energy and Buildings 2000;34:103–9.
[12] Papalambros PY, Wilde DJ. Principles of optimal design: modeling and computation. Cambridge University Press: Cambridge, New York; 2000.
[13] Edgar TF, Himmelblau DM, Lasdon LS. Optimization of chemical processes. McGraw-Hill: Boston; 2001.
[14] TRNSYS: a transient simulation program reference manual. Solar energy laboratory, University of Wisconsin-Madison, 1996.
[15] VisualDOE3.0 program documentation, San Francisco, USA: Eley Associates; 2001.
[16] Lebrun J, Bourdouxhe JP, Grodent M. HVAC1KIT: a toolkit for primary HVAC system energy calculation. ASHRAE, TC 4.7 energy calculation, 1995.
[17] Fletcher R. Practical methods of optimization. Chichester, New York: Wiley; 2001.
[18] Kelley CT. Iterative methods for optimization. Philadelphia, PA: SIAM; 1999.